ASSESSMENT OF CREEP-FATIGUE DAMAGE USING THE UK STRAIN BASED PROCEDURE

S.K. BATE
AEA Technology plc,
Plant Support Services,
Risley, Warrington,Cheshire,
United Kingdom

Abstract

The UK strain based procedures have been developed for the evaluation of damage in structures, arising from fatigue cycles and creep processes. The fatigue damage is assessed on the basis of modelling crack growth from about one grain depth to an allowable limit which represents an engineering definition of crack formation. Creep damage is based up on the exhaustion of available ductility by creep strain accumulation. The procedures are applicable only when level A and B service conditions apply, as defined in RCC-MR or ASME Code Case N47. The procedures require the components of strain to be evaluated separately, thus they may be used with either full inelastic analysis or simplified methods. To support the development of the UK strain based creep-fatigue procedures an experimental program was undertaken by NNC to study creep-fatigue interaction of structures operating at high temperature. These tests, collectively known as the SALTBATH tests considered solid cylinder and tube-plate specimens, manufactured from Type 316 stainless steel. These specimens were subjected to thermal cycles between 250°C and 600°C. In all the cases the thermal cycle produces tensile residual stresses during dwells at 600°C. One of the tube-plate specimens was used as a benchmark for validating the strain based creep fatigue procedures and subsequently as part of a CEC co-operative study. This benchmark work is described in this paper. A thermal and inelastic stress analysis was carried out using the finite element code ABAQUS. The inelastic behaviour of the material was described using the ORNL constitutive equations. A creep fatigue assessment using the strain based procedures has been compared with an assessment using the RCC-MR inelastic rules. The analyses indicated that both the UK strain based procedures and the RCC-MR rules were conservative, but the conservatism was greater for the RCC-MR rules.

1. INTRODUCTION

To support the development of the UK strain based creep-fatigue procedures[1] an experimental program was undertaken by NNC to study creep-fatigue interaction of structures operating at high temperature. These tests, collectively known as the SALTBATH tests considered solid cylinder and tube-plate specimens, manufactured from Type 316 stainless steel. These specimens were subjected to thermal cycles between 250°C and 600°C. In all the cases the thermal cycle produce tensile residual stresses during dwells at 600°C.

One of the tube-plate specimens was used as a benchmark for validating the strain based creep fatigue procedures. The benchmark work is described in this paper. A thermal and inelastic stress analysis was carried out using the finite element code ABAQUS[2]. The inelastic behaviour of the material was described using the ORNL constitutive equations[3].

A creep fatigue assessment using the strain based procedures has been compared with an assessment using the RCC-MR elastic and inelastic rules.

This benchmark was subsequently used in a CEC co-operative exercise in the simulation of an experiment[4]. The predictions of inelastic calculations using various constitutive equations and non-linear finite element programs are compared. Some of these results were then used in a further CEC benchmark exercise on laws for damage assessment[5]. The predictions of the UK strain based method and RCC-MR are shown.

2. DESCRIPTION OF BENCHMARK

The specimen used for the benchmark was identified as a 'Type 2 Saltbath specimen' and is shown in Figure 1. The right-hand side (as shown in the figure), in particular the region around the 5mm radius, is intended to represent a typical geometrical feature of a tube-tubeplate junction. The left-hand side is a removable plug, allowing periodic inspection of the interior surface, and is not intended to be of structural significance.

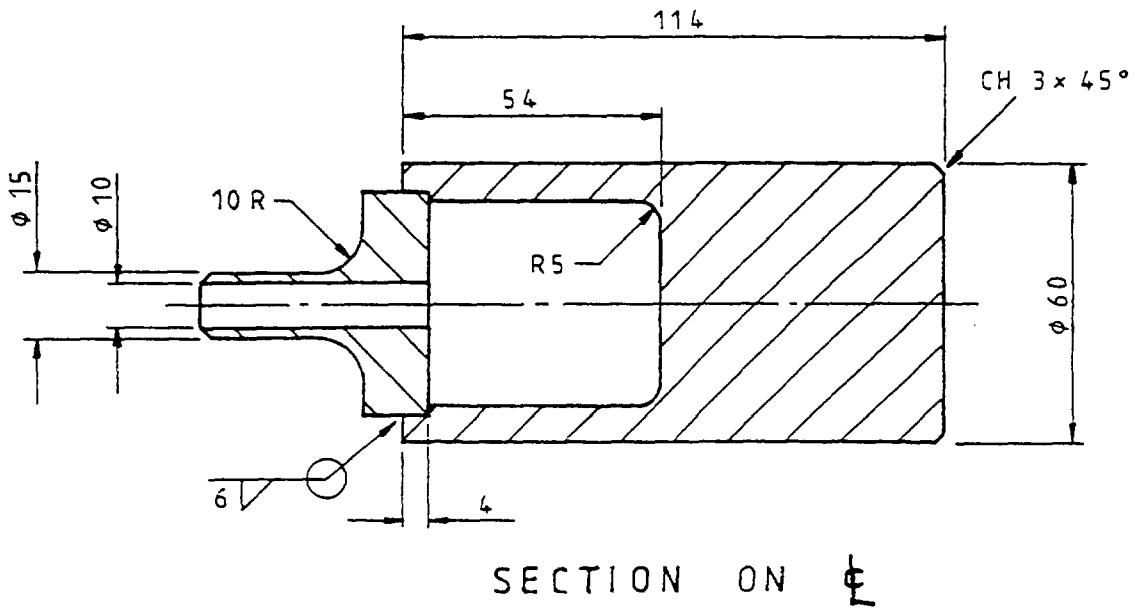

CYCLE DESCRIPTION

Step	Event
0	Initial condition - Uniform Temperature 600°C
1	Immerse in heat treatment salt at 250oC fro 30 seconds (step change in fluid temeprature). Heat transfer coefficient on external surfaces 3000 W/m2K. Internal surfaces adiabatic
2	Heat in air, fluid temperature 600oC. Heat transfer coefficient 80 W/m2K on external surfaces. Internal surfaces adiabatic.
3	Hold at uniform temperature of 600oC for 15 hours
4	As step 1

Note

The design of this testpiece is such that discontinuity stresses at each end of the chamber have decayed to low levels at the mid length of the chamber.

FIG. 1. Geometry of Tube-Plate Test Piece (Type 2) [7]

For the benchmark problem, the applied thermal cycle was a thermal downshock from 600°C to 250°C for 30 seconds, followed by heating at 600°C for one hour to attain a uniform temperature before a hold time of fifteen hours at 600°C. The thermal shocks were applied by immersing the specimens in heat treatment salt and then slowly re-heating in air to attain a uniform temperature at the dwell period.

3. FINITE ELEMENT ANALYSES

The specimen has been modelled using eight noded axisymmetric elements with symmetry conditions applied, see Figure 2. The finite element program ABAQUS was used for the analyses. The desired mesh refinement was obtained after making several elastic analyses and validating the results with those obtained in a previous analysis[6].

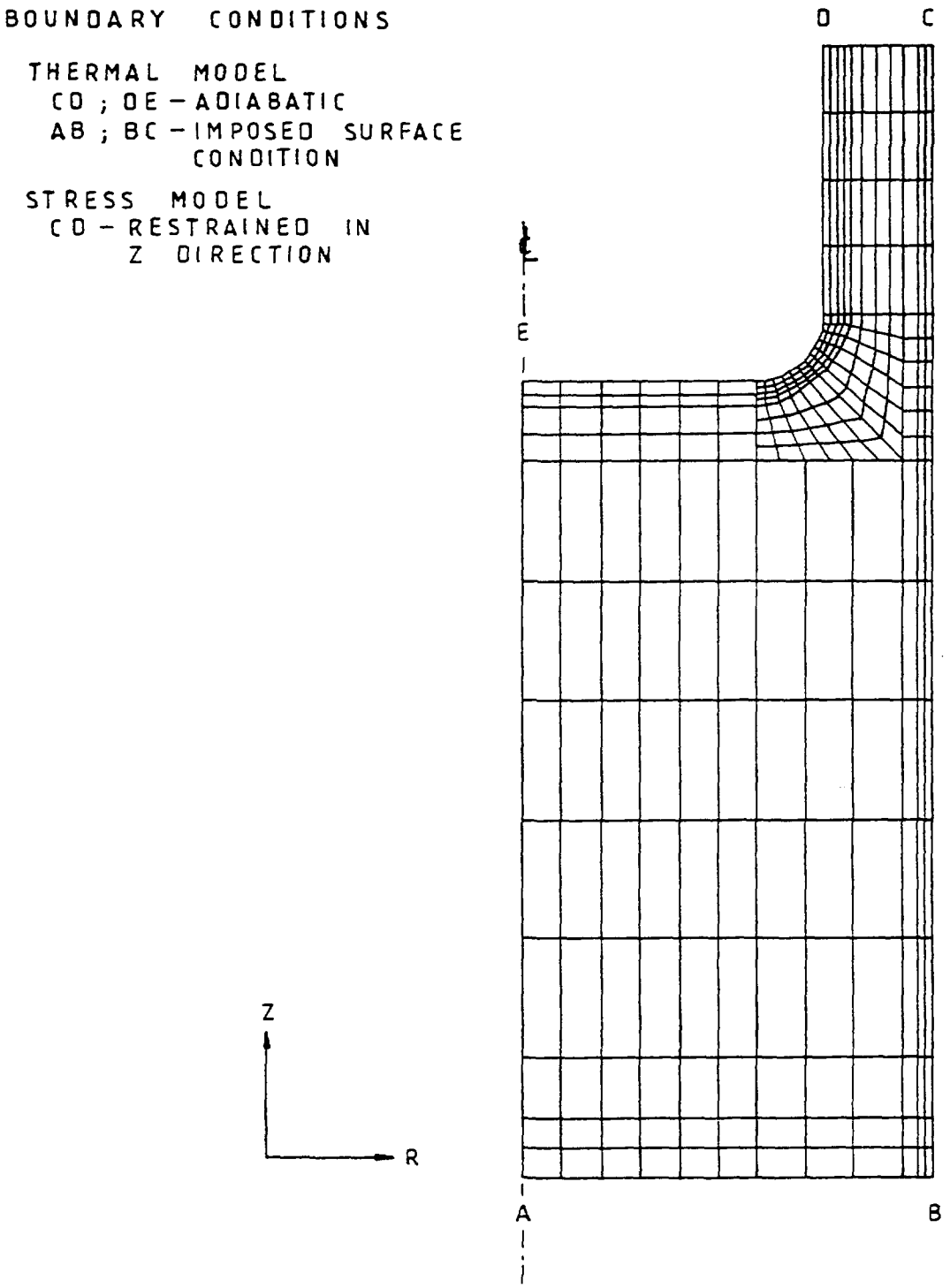

FIG.2. Finite Element Model and Boundary Conditions Applied

The finite element analysis consisted of :

(a) A thermal analysis (using ABAQUS DCAX8 elements): For the thermal cycle described previously a thermal analysis was completed and the results written to file to be used for the subsequent stress analyses.

(b) Inelastic Stress Analyses (using ABAQUS CAX8R reduced integration elements): Two cases were considered to examine the sensitivity of the ORNL constitutive equations with different plasticity parameters. Note, the parameters normally recommended for use with the ORNL constitutive equations are based upon 10th cycle data.

CASE 1 - This was based upon the 100th cycle curve[7]. An elastic-plastic slope was drawn based upon the slope of the curve and the yield stress was derived from the intersection of the elastic plastic slope with the elastic slope. The plastic slope required in ABAQUS was derived from these values.

The analysis used the alpha reset option and all the parameters were temperature independent. The initial and cyclic properties were assumed identical.

CASE 2 - This was also based upon the 100th cycle curve but an elastic-plastic slope based on the 10th cycle curve was used. The yield stress was derived by the intersection of the elastic and elastic plastic slope. The same conditions as case 1 were then assumed.

4. RESULTS OF THE ANALYSES

The rapid thermal loading of the outside surface can be seen in Figure 3. This leads to yielding of the whole area of this surface within a second of the downshock. There is also a small amount of yielding at the fillet. The faster cooling of the tube relative to the plate section leads to bending at the fillet section, see Figure 4.

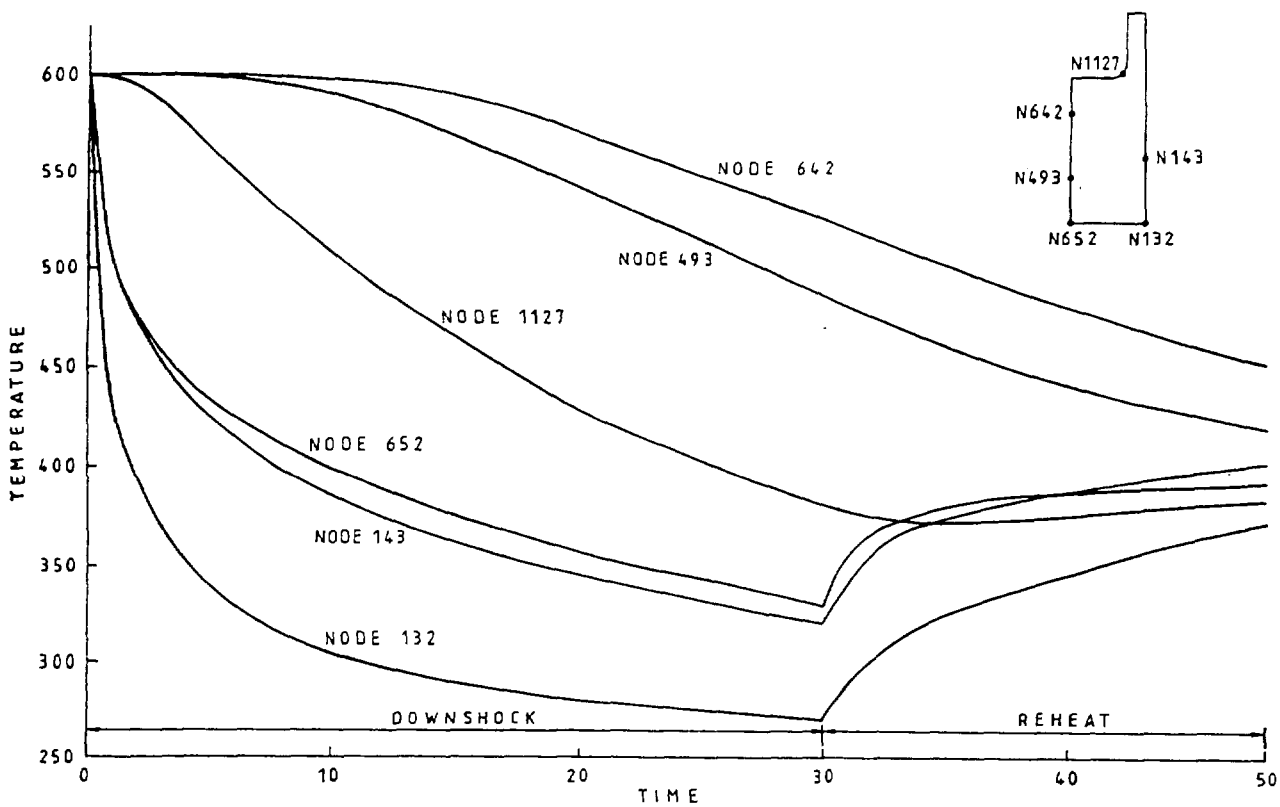

FIG. 3. Plot of Temperature against Time

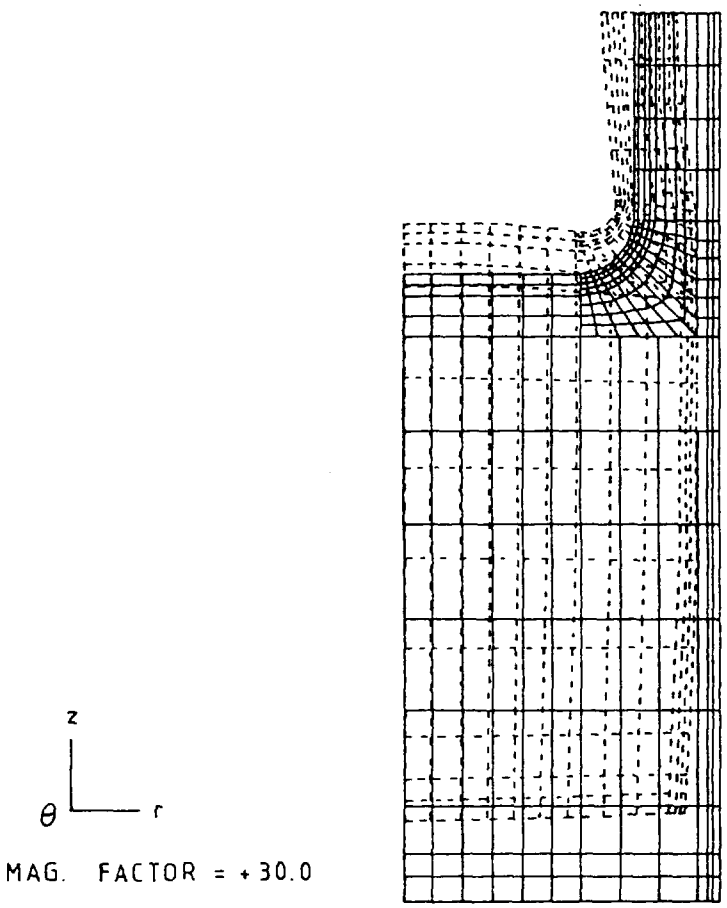

FIG. 4. Displacement Plot

Figure 5 shows the results obtained after five stress/strain cycles have been applied for CASE 2. The principal stress histories at the peak stress position are shown for the two cases in Figures 6 and 7. Figure 8 shows a hysteresis plot of the equivalent (Mises) stress and strain.

The results indicate that in the first second of the transient significant 'skin' stresses occur in the specimen. Shortly after this time, the plastic strain at the fillet accumulates as the secondary stresses start to dominate. This effect can be seen in the principal stress histories at the fillet. These figures show that the principal stress tangential to the fillet dominates throughout the cycle except at unloading. Both CASES indicate that through-wall yielding occurs at the fillet and all the outside surface. They show a peak stress at the fillet 15 seconds into the transient. The magnitude and distribution of inelastic strain within the specimen is dependent on the material parameters used in the ORNL constitutive equations.

The results of this analysis were compared in a CEC benchmark exercise between six participants, each using different combinations of constitutive equations and non-linear finite element programs. These combinations are shown in Table I with the predictions of strain range at a point where it is maximised.

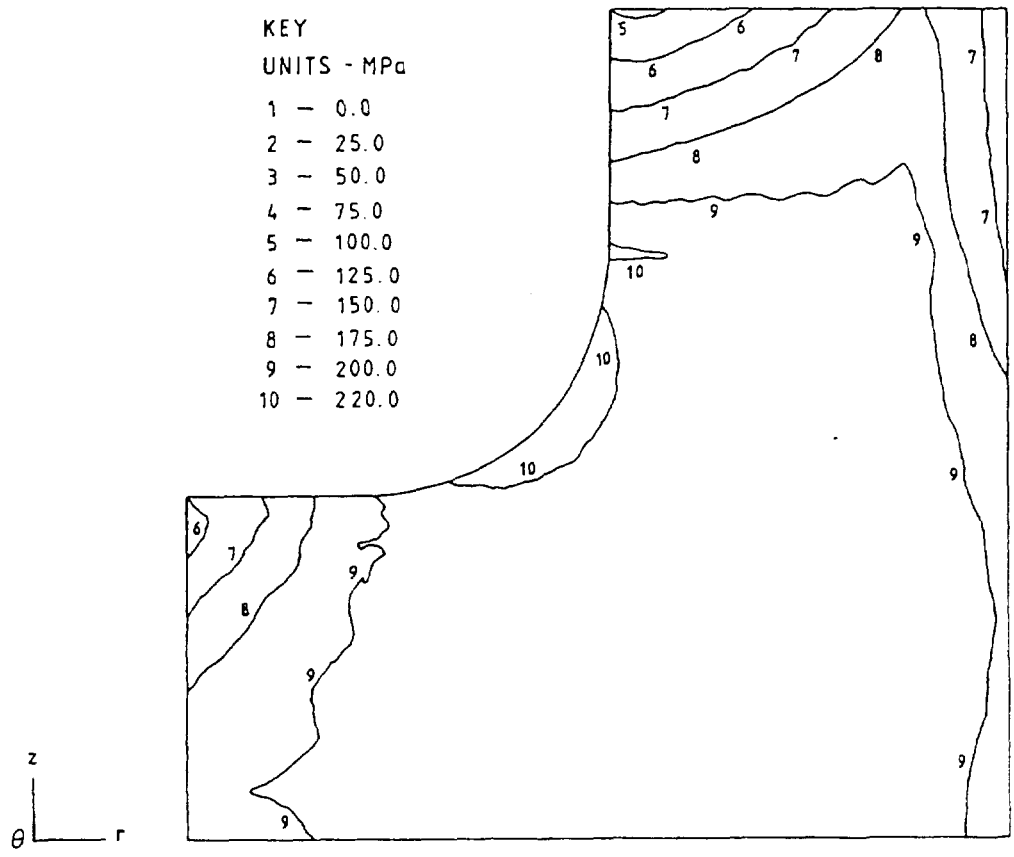

FIG. 5a. Von Mises Stress Distribution / Peak Stress at Fillet During Sixth Operational Cycle, CASE 2

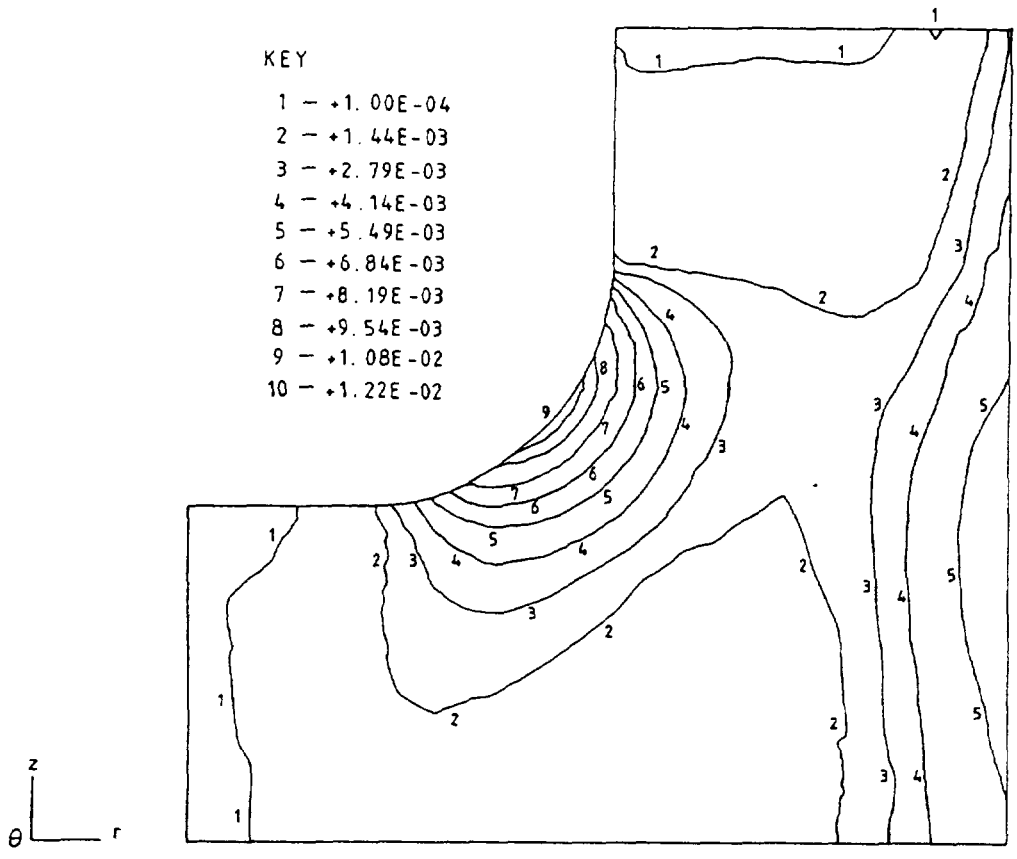

FIG. 5b. Plastic Strain Magnitude / Peak at Fillet During Sixth Operational Cycle, CASE 2

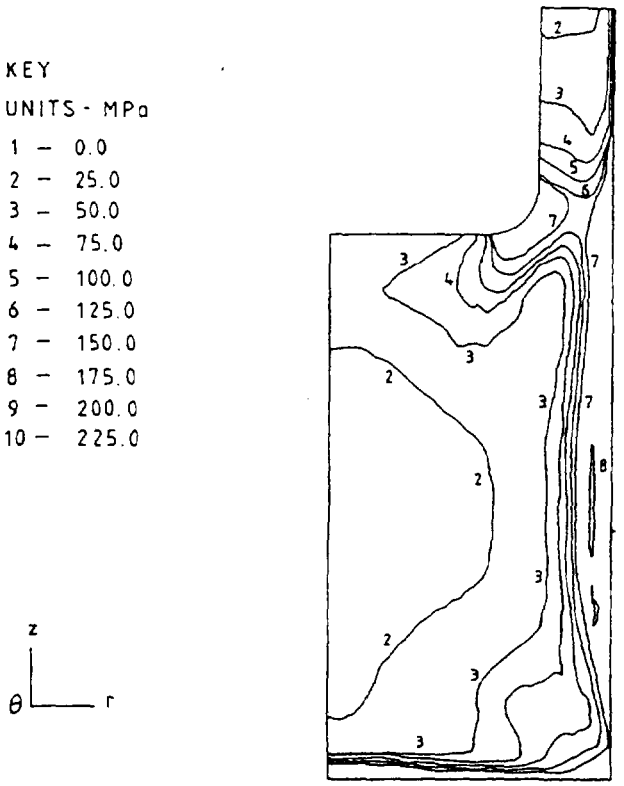

FIG. 5c. Von Mises Stress Distribution / At End of Reheat During Sixth Operational Cycle, CASE 2

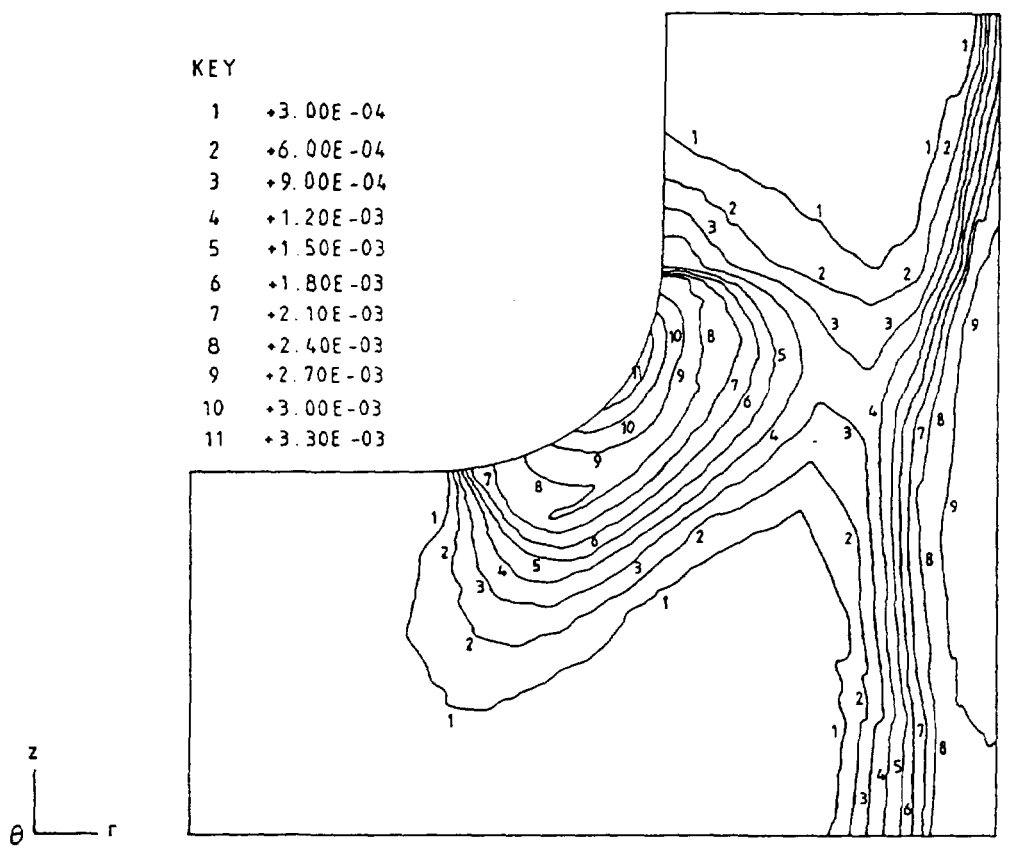

FIG. 5d. Creep Strain Magnitude After Five Cycles (Total Hold Time = 75 hours), CASE 2

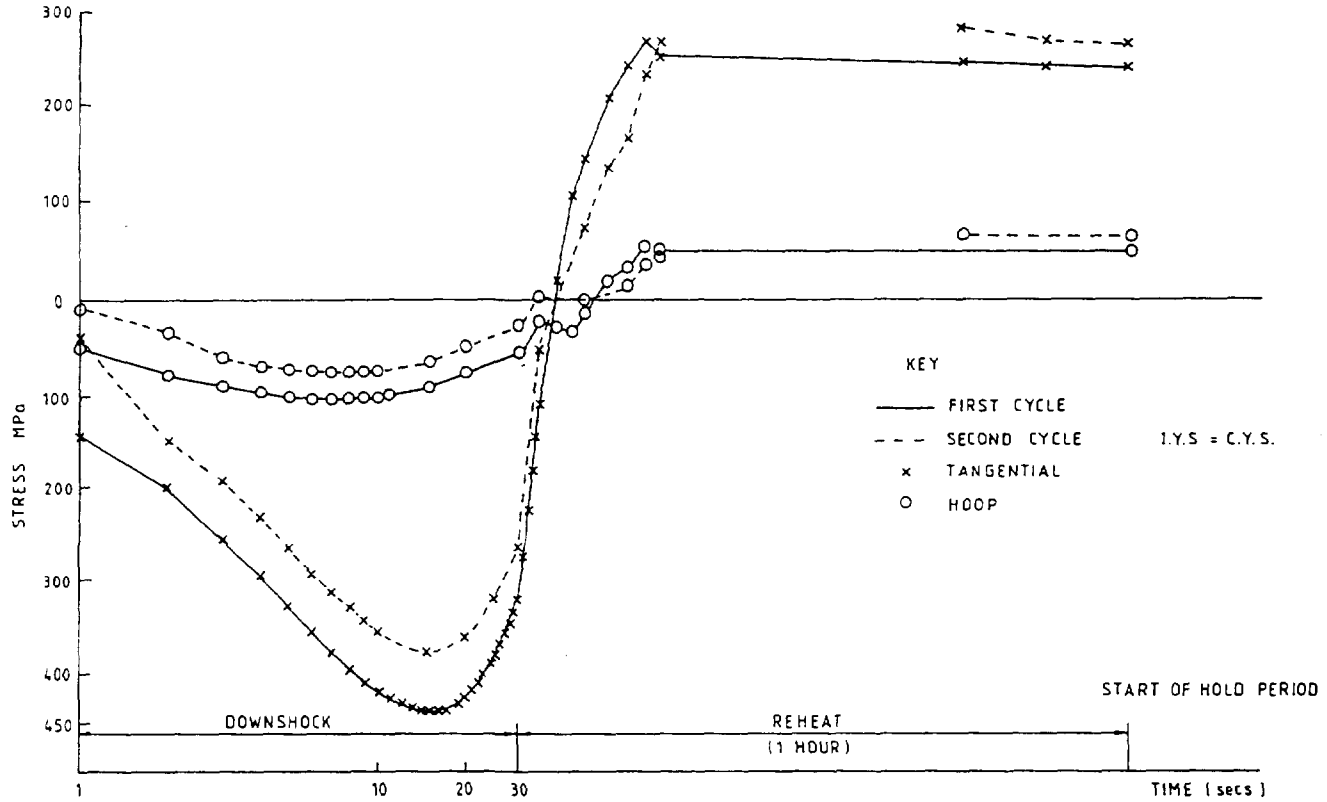

FIG. 6. Principal Stress History Over Downshock and Reheat (Using Hundreth Cycle Data Hundreth Cycle Plastic Slope)

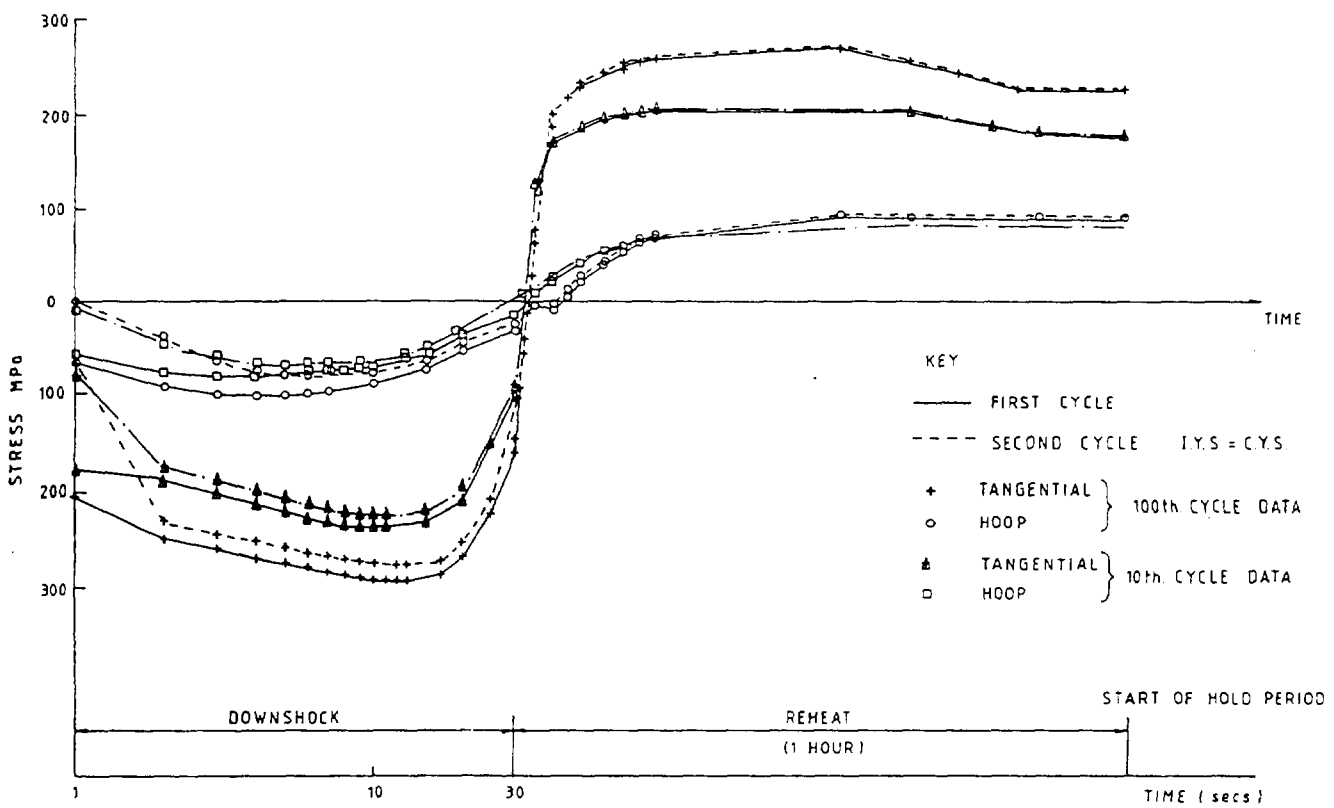

FIG. 7. Principal Stress History Over Downshock and Reheat (Using Hundreth Cycle Data Tenth Cycle Plastic Slope)

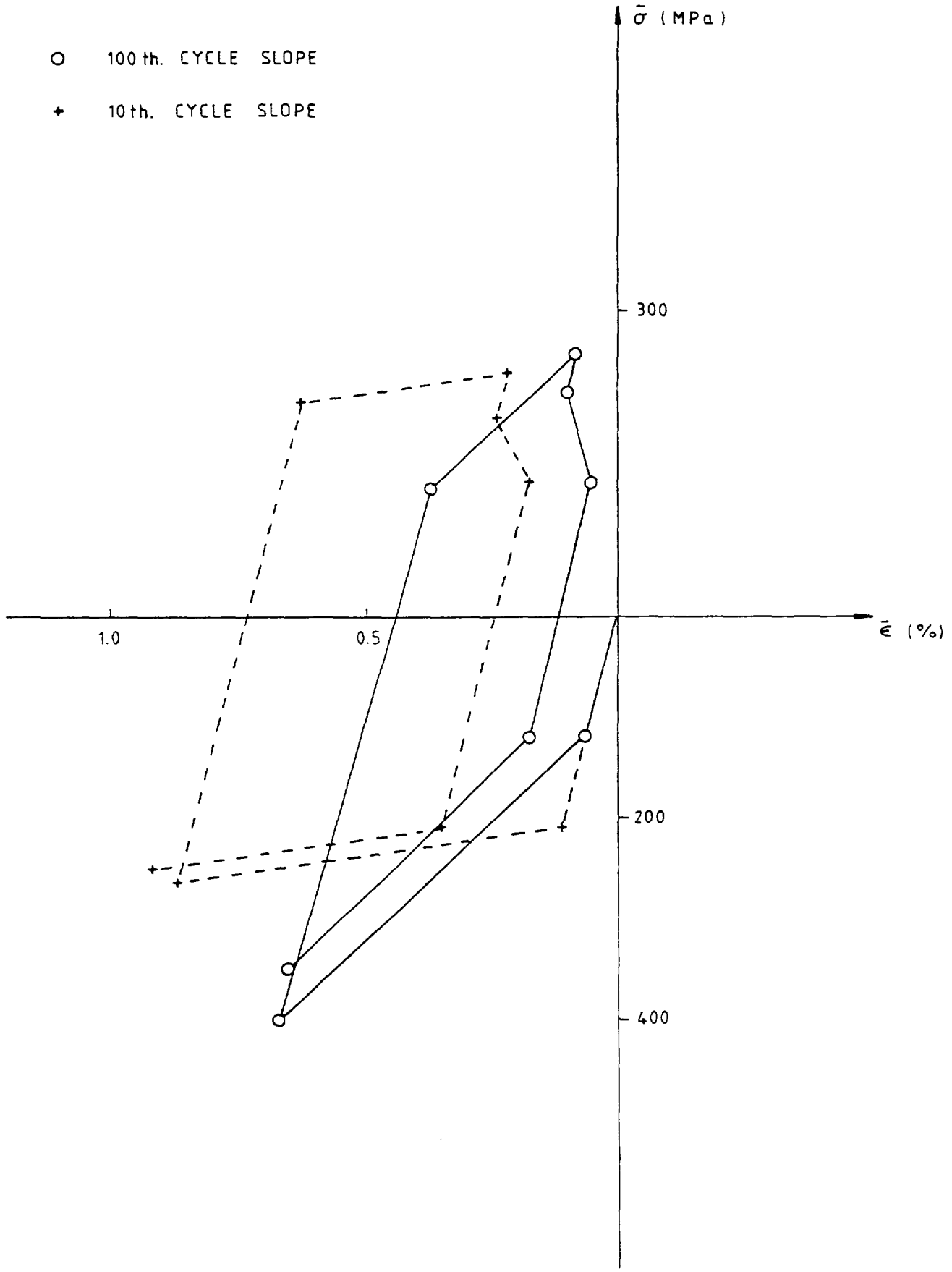

FIG. 8. Stress-Strain Hysteresis Loop (Using Hundreth Cycle Curve)

TABLE I. STRAIN RANGES IN % AT MAXIMUM POINT [4]

FE CODE	MATERIAL MODEL		CYCLE					
			1	2	3	4	5	6
ABAQUS	ORNL	CASE 1	0.612				0.6014	
		CASE 2	0.748				0.7157	
ABAQUS	Fast Reactor State Variable		0.724	0.623	0.607	0.599	0.594	0.590
ANSYS	Bilinear Kinematic		0.63	0.63	0.63	0.63	0.63	
ABAQUS	Interatom		0.943	0.963	0.916	0.918	0.922	
SYSTUS	Chaboche		0.87	0.79	0.87	0.74	0.72	0.78
INCA	Chaboche		0.688	0.649	0.627			

Four solutions agreed fairly closely with a steady state maximum strain range of about 0.6%. Two further solutions had values of about 0.72% and one solution 0.9%. Examination of the results suggested that the reason for the differences lay in the basic test data used to form material parameters.

Further comparison was made of the equivalent stress at four positions of the stress strain cycle: maxima during the downshock and reheat, and values at the start and end of the hold period. These results are shown in Table II.

TABLE II. VON MISES EQUIVALENT STRESSES (MPa): MAXIMA DURING DOWNSHOCK AND REHEAT, VALUES AT START AND END OF HOLD PERIOD [4]

FE CODE	MATERIAL MODEL	STAGE	CYCLE			
			1	3	5/6	12
ABAQUS	ORNL CASE 2	Downshock			250	
		Reheat			240	
		Start of Hold			197.3	
		End of Hold			160.6	
ABAQUS	Fast Reactor State Variable		178.2	234.8	250.1	263.7
			220.1	220.0	221.4	223.8
			220.1	220.0	221.4	223.8
			130.3	148.6	159.9	172.3
ANSYS	Bilinear Kinematic		314.0	331.0	346.0	
			137.0	123.0	108.0	
			84.9	72.8	61.1	
			76.9	65.4	54.4	
ABAQUS	Interatom		166.4	178.6	176.6	
			161.0	181.7	193.3	
			148.0	170.3	184.3	
			138.2	160.2	174.0	
SYSTUS	Chaboche				207.6	
					210.2	
					-	
					113.6	
INCA	Chaboche		195.3	244.1		
			180.1	239.1		
			-	-		
			132.3	177.8		

The results in Table II show, apart from the analysis using the bilinear kinematic model, a spread of up to 25% over all the stages. The most important aspect concerns the hold period when most of the time dependent (creep) damage is to be expected. The exact damage comparison would be dependent upon the specific damage rule used. This is related to in the next section where damage laws are compared.

Similar differences are also evident for the amount of relaxation. It is thought likely that the substantial differences are due to discrepancies in the underlying material data related to the creep tests.

5. CREEP FATIGUE DAMAGE ASSESSMENT

Using the UK strain based rules and RCC-MR[8] creep-fatigue rules an estimate of the design life has been based upon the results obtained after five cycles had been applied. Due to the effects of stress relaxation and creep a stable cycle had not been obtainable but the difference between each stress strain cycle was not causing a considerable difference in the life predicted by each cycle.

The estimates of design life are shown in Table III.

TABLE III. COMPARISON OF DESIGN LIFE PREDICTIONS

CASE	UK Strain Based Method				RCC-MR			
	Strain Range (%)	Fatigue Damage /Cycle	Creep Damage /Cycle	Allowable Design Cycles	Strain Range (%)	Fatigue Damage /Cycle	Creep Damage /Cycle	Allowable Design Cycles
1	0.7189	0.00128	0.00814	78	0.6014	0.0027	0.1098	9
2	0.8347	0.00214	0.00573	46	0.7157	0.004	0.0451	18

Notes: 1. UK procedures use Rankine strain range to evaluate fatigue damage

2. RCC-MR procedures use Von Mises strain to evaluate fatigue damage.

For CASE 1, a prediction of 78 cycles was obtained using the UK procedure whereas CASE 2 predicted a life of 46 cycles. This difference is due to the strain range (hence fatigue damage) predicted by each case. The difference in the amount of creep damage has no effect in the UK method but RCC-MR predicts a reduction in life due to the increased creep damage.

Further comparison can be drawn from the CEC benchmark exercise[5] where results from several of the inelastic analyses completed in Section 4 were used to evaluate creep fatigue damage using the UK strain based method and the RCC-MR rules. The predicted design life is shown in Table IV.

No cracks had been observed in the experimental specimens after 280 cycles. The results therefore indicate that both procedures, with the exception of the Chaboche and UK strain based method, provide a conservative estimate of the design life, with the UK strain based method providing a less conservative estimate.

The results show that the predicted failure can differ greatly depending on the constitutive model used. The main difference in this case being caused by the predicted stresses and strains during the steady state (creep) period. The creep damage assessment which is based on the viscoplastic strain for the strain based method was generally less severe than the stress based method of RCC-MR. The creep

TABLE IV. PREDICTED DESIGN LIFE USING VARIOUS CONSTITUTIVE MODELS [5]

Constitutive Model	Damage Assessment Model					
	UK Strain Based Method			RCC-MR		
	Cycles to Failure	Fatigue Damage per Cycle	Creep Damage per Cycle	Cycles to Failure	Fatigue Damage per Cycle	Creep Damage per Cycle
Interatom	177	5.65×10^{-3}	1.20×10^{-4}	48	1.24×10^{-2}	3.59×10^{-3}
Chaboche (SYSTUS)	473	2.11×10^{-3}	1.59×10^{-5}	71	6.25×10^{-3}	3.33×10^{-3}
ORNL CASE 2	46	2.15×10^{-3}	5.73×10^{-3}	18	4.13×10^{-3}	4.51×10^{-2}

damage per cycle was found to be negligible with the unified constitutive models (Interatom and Chaboche model. On the contrary, the non-unified ORNL model, the strain was non negligible and hence creep damage was more significant.

The other significant comparison came from the predicted mechanism governing damage. For the strain based damage law, the unified constitutive models predicted pure fatigue cracks, whereas the ORNL model predicted creep fatigue interaction.

Using the RCC-MR damage law, creep fatigue cracks were predicted in all three cases, with, however dominating creep damage for the ORNL model and dominating fatigue damage for the Interatom model. Unfortunately none of the specimens have been tested until crack initiation and these differences can not be checked.

6. CONCLUDING REMARKS

The conclusions of this analysis are reflected by the CEC benchmark studies and therefore it is worthy that some of the conclusions from these studies are reiterated here.

Constitutive Equations:

The simple kinematic model of plasticity, though agreeing with several other models with respect to strain range, gave very discrepant results for stresses at extreme stages of the cycle, including the hold period, and also in the distributions of stresses at different stages. This is considered to arise principally from an inappropriate relation between mean stress and stain in cycling. The model is therefore not recommended for other severe thermally loaded problems involving creep.

In view of the differences arising from use of different material data the value of comparison is reduced. Clearly a consistent base of raw data should be obtained for refitting of all constitutive equations intended for future use and development.

Damage Models:

Both the strain based and RCC-MR models appear to be conservative.

A characteristic feature is that the unified constitutive models predict a pure fatigue failure mechanism whilst the non-unified ORNL model predicted a creep-fatigue mechanism. The differences in the predicted stresses and strains during creep meant that the unified models generally predicted lower creep damage than the non-unified models.

REFERENCES

[1] PICKER, C., "UK Development of a Strain-Based Creep Fatigue Assessment Procedure for the Evaluation of Creep and Fatigue Damage in Fast Reactor Design", IAEA Technical Committee Meeting on Creep Fatigue Damage Rules to be Used in Fast Reactor Design, Manchester (1996)

[2] HIBBIT, D et al., ABAQUS Version 4.7

[3] CORUM, J.M., "Interim Guidelines for Detailed Inelastic Analysis of High Temperature Reactor System Components", ORNL-5014.

[4] WHITE, P.S., "A Co-operative Benchmark Exercise in the Simulation of an Experiment - Inelastic Analysis of Type 2 SaltBath Specimens", CEC Contract Number RA1.0161.UK.

[5] CABRILLAT, M.T., "Benchmark on Laws for Damage Assessment", CEC Contract Number RA1.CT91.0195

[6] BESTWICK, R.D.W., HUGHES, P.M., "Development of a Tube-Tubeplate Testpiece for use in the Saltbath Creep-Fatigue Test Programme", UK Fast Reactor Document

[7] BESTWICK, R.D.W., BUCKTHORPE, D.E., "Data for use in Assessments of Saltbath Creep Fatigue Tests", UK Fast Reactor Document

[8] RCC-MR Addendum No. 1 - November 1987